

The Music of the Sphere: Inferring the 3D Gravitational Potential of the Universe on the Largest Scale from Cosmic Microwave Background Observations

Roger D. Blandford,^{1*} Philip J. Marshall,¹ Laurence Perrault Levasseur¹

¹*Kavli Institute for Particle Astrophysics and Cosmology, Stanford University, 452 Lomita Mall, Stanford, CA 94035, USA*

to be submitted to arxiv

ABSTRACT

Abstract goes here.

Key words: cosmology

1 OVERVIEW

Observations of temperature fluctuations in the CMB measure the 2D potential Φ (considered as a linear perturbation to the Robertson-Walker metric tensor under the Newtonian gauge) on the sphere of last scattering (where the scale factor $a \sim 0.0009$ and the time is $t \sim 380$ kyr). The measurement is quite direct on large angular scale ($\ell \lesssim 30$) in the “Sachs-Wolfe” regime; it is indirect on small angular scales where velocity and density perturbations are more important, which are linearly related to the potential perturbation. It is also possible, at least in principle, to learn about the first and second radial derivatives of this potential through studying the polarization. This 2D potential is derived from a 3D potential which fills the sphere and extends beyond our horizon. This potential is derived from one specific realization of an initial Fourier spectrum of inferred type and statistical properties. This paper reports on an investigation of what can be learned, at least in principle, about the 3D potential at the time of recombination from the 2D information. Furthermore, any set of Fourier components can be evolved assuming the now standard “Flat Λ CDM” cosmology and connected to the potential information derivable from large surveys conducted out to modest redshift. What is being discussed here is an exercise in basic cartography and not in measuring the physical behavior of the universe at either early or late times. As with many such exercises the goal is to understand the approximate arrangement of structure within the observable universe on the largest linear scales. We shall be more concerned with the topological organization of this structure than with precise measurement. However, success in this endeavor ought to improve the investigation of physics questions through contributing constraining priors to Bayesian inference studies.

In Sec. 2, we discuss the basic assumptions that we will

make in our idealized versions of the problem. This is followed in Sec. 3 by a description of the Fourier representation of the 3D potential and its relationship to the spherical harmonic decomposition on the last scattering sphere. The nesting of equipotential contours on the last scattering photosphere is analyzed in Sec. 4 and this is generalized to surfaces in 3D in the following section. The relationship between the 2D and 3D equipotentials is discussed in Sec. 6. In Sec. 7., we outline a Bayesian approach to calculating the likeliest form of the 3D potential, paying special attention to the criteria which dictate the effective resolution of the reconstruction and how this may be improved by adding interior data. Our conclusions are collected in Sec. 8. A future publication will apply this approach to actual data.

2 BASIC ASSUMPTIONS

We work with an idealized problem which we specify as follows:

- Represent the big bang as a sphere of comoving radius ~ 14.23 Gpc (adopting a Hubble constant of $68 \text{ km s}^{-1} \text{ Mpc}^{-1}$) and flat Λ CDM. The last scattering surface – the *cosmic photosphere* – is a sphere with radius ~ 0.29 Gpc smaller. Recombination occurs over a short but finite interval of time just prior to last scattering. The radius of the cosmic photosphere, 13.94 Gpc, is our unit of length.
- Ignore the expansion of the universe and just consider the potential as a set of linear normal modes at the time of last scattering. These can be evolved backward and forward in time with confidence. In practice, the potential changes little after recombination although shorter-wavelength modes eventually become nonlinear. (This, too, can be accommodated in principle.)
- Consider only scalar modes, setting the tensor contribution to zero. If, one day, a significant tensor component is

* rdb3@stanford.edu

confidently measured, minor modifications to what follows can be included.

- Hypothesize that the amplitude of each of these modes is drawn from a Gaussian distribution with zero mean, random phase and initial variance roughly proportional to k^{-3} as is consistent with the observations.

- Ignore modes with wavelength longer than the side of the box, L . Their contributions can be approximately incorporated into the lowest Fourier components in a given box as long as we only care about observations within our horizon. This procedure will improve as we enlarge the box. However if the box is too large the spacing of modes in k -space $\Delta k = 2\pi/L$ will be too fine and the amplitudes of neighboring modes will be poorly distinguished. A choice $L \sim 4$ turns out to be a good compromise. Truncate the spectrum with a sphere of radius $n_{\max}\Delta k$; shorter wavelength modes contribute to the error and a Gaussian window function may be preferable.

3 FOURIER MODES

We represent the potential Φ within the box in polar coordinates as a Fourier series with wave vectors $\mathbf{k} = \Delta k\{n_1, n_2, n_3\}$, with n_1, n_2, n_3 integers and $\Delta k = 2\pi/L$. As Φ is real, we only need to assign one real number to each mode. We approximate Eq. (1) by a finite sum restricted to $(n_1^2 + n_2^2 + n_3^2)^{1/2} \leq n_{\max}$ and we label the coefficients $f_{\mathbf{k}}$ by the index n running from 1 to $N \sim 4\pi n_{\max}^3/3$. ($N = 6, 32, 122, 256, 514, 924, 1418, 2108, 3070, 4168$ for $n_{\max} = 1$ through 10.) It is simplest to restrict \mathbf{k} to a hemisphere and to write:

$$\Phi[\mathbf{x}(x, \theta, \phi)] = \sum_{n=1}^{N/2} [f_n \cos(\mathbf{k}_n \cdot \mathbf{x}) + f_{N+1-n} \sin(\mathbf{k}_n \cdot \mathbf{x})] \quad (1)$$

Our main goal is to relate surface information on the photosphere to the underlying f_n .¹ The approach that we will follow is constructive. Φ can be expanded exactly as an infinite sum of Legendre polynomials which we truncate at a finite value of ℓ , starting with $\ell = 1$.

$$\Phi(\mathbf{x}; \ell) = \sum_{\ell'=0}^{\ell} (2\ell'+1) \sum_{n=1}^N j_{\ell'}(k_n x) P_{\ell'}(\hat{\mathbf{k}}_n \cdot \hat{\mathbf{x}}) \mathcal{S}(n, \ell') f_n, \quad (2)$$

where $\mathbf{k}_n = \mathbf{k}_{N+1-n}$ and $\mathcal{S}(n, \ell) = [\cos(\ell\pi/2), \sin(\ell\pi/2)]$, for $[1 \leq n \leq N/2, N/2 < n \leq N]$. As ℓ is increased the effective resolution of Φ , in radius and angle, improves. It is convenient to treat ℓ as a continuous variable by the device of summing up to $[\ell]$ and then adding the next term in the sum multiplied by $(\ell - [\ell])$. To describe the potential generated by modes with a given value of n_{\max} , we need spherical harmonics up to $\ell \sim 3n_{\max}$ and *vice versa* (Fig. 1). An immediate implication is that an accurate Φ map on the sphere, degraded to resolution ℓ provides $L = (\ell - 1)(\ell + 3)$ real numbers which can be used to solve for N real Fourier coefficients suggesting that there is enough information in a $\ell = 9$ map to solve for ~ 100 Fourier components up to $n_{\max} \sim 3$ independent of the priors on their actual values.

¹ This is sometimes called *holography*, though it is not the original meaning of the word.

When we include the priors, we can proceed to finer scale. Also, when we reduce the radius of the sphere, the value of n_{\max} probed by a given ℓ scales $\propto x^{-1}$ (Fig. 2).

4 RELATING SURFACE AND INTERIOR EQUIPOTENTIALS

Now let us outline how to extract information about the interior potential from the surface potential. We suppose that we are in the Sachs-Wolfe region of the spectrum where the surface potential $\Phi(1, \theta, \phi) = 3\delta_T$, where δ_T is the relative CMB fluctuation. We set aside for the moment the velocity and density contributions to the observed fluctuation and the additional information (roughly twice as much) that can be garnered from adding polarization maps. We align the 3 axis (Eq. (1)) with $\theta = 0$ and the 1 axis with $\phi = 0$.

Our first task is to describe the inferred potential on the sky. We suppose this is approximated by a finite sum over spherical harmonics:

$$\Phi(1, \theta, \phi; \ell_{\max}) = \sum_{y=1}^{(\ell_{\max}+1)^2} a_y Y_y(\theta, \phi), \quad (3)$$

where $Y_y = \{Y_{0,0}, Y_{1,0}, 2^{1/2}\Re[Y_{1,1}], 2^{1/2}\Im[Y_{1,1}], Y_{2,0}, \dots, 2^{1/2}\Im[Y_{\ell_{\max}, \ell_{\max}}]\}$. Note that there are $2\ell + 1$ independent, real, basis function in each ℓ -shell. Note also that $\int d\Omega Y_y Y_{y'} = \delta_{yy'}$.

Next, we describe the potential using Eq. (2) and the identity

$$P_{\ell}[\hat{\mathbf{k}}(\theta', \phi') \cdot \hat{\mathbf{x}}(\theta, \phi)] = \frac{4\pi}{2\ell+1} \sum_{y=\ell^2+1}^{(\ell+1)^2} Y_y(\theta', \phi') Y_y(\theta, \phi) \quad (4)$$

The spherical harmonic coefficients are then given by the linear relation

$$a_y = \mathbf{R}_{yn} f_n, \quad (5)$$

where we adopt the summation convention and

$$\mathbf{R}_{yn} = 4\pi i^{\ell} Y_y^*(\theta', \phi') j_{\ell}(k), \quad (6)$$

with $\cos \theta' = n_3/n$, $\tan \phi' = n_2/n_1$. The elements of the transformation matrix \mathbf{R}_{yn} have been tabulated up to $n_{\max} = 6$, $\ell = 10$ which should be sufficient for our purpose.

We estimate the importance of spherical harmonics with order ℓ to the signal at a given given range of k by evaluating the sum:

$$P(\ell; n_{\max}) = \sum_{n=N(n_{\max}-1)+1}^{N(n_{\max})} \sum_{y=\ell^2-3}^{(\ell-1)(\ell+2)} |\mathbf{R}_{yn}|^2 \quad (7)$$

5 INFERRING THE 3D POTENTIAL

Our task is to take a given vector of measured spherical harmonic coefficients \mathbf{a} , with covariance matrix C , and infer a vector of the Fourier coefficients of our model potential, \mathbf{f} , under the prior assumption that the components f_n are independent and drawn from a Gaussian distribution with variance $\sigma_n^2 = (n_1^2 + n_2^2 + n_3^2)^{-3/2}/\alpha$. We seek the posterior PDF $\mathcal{P} = \Pr(\mathbf{f}|\mathbf{a}, \alpha)$, where

$$-\ln \mathcal{P} = (\mathbf{a} - \mathbf{R}\mathbf{f})^T C^{-1} (\mathbf{a} - \mathbf{R}\mathbf{f}) + \mathbf{f}^T S^{-1} \mathbf{f} + \text{const.} \quad (8)$$

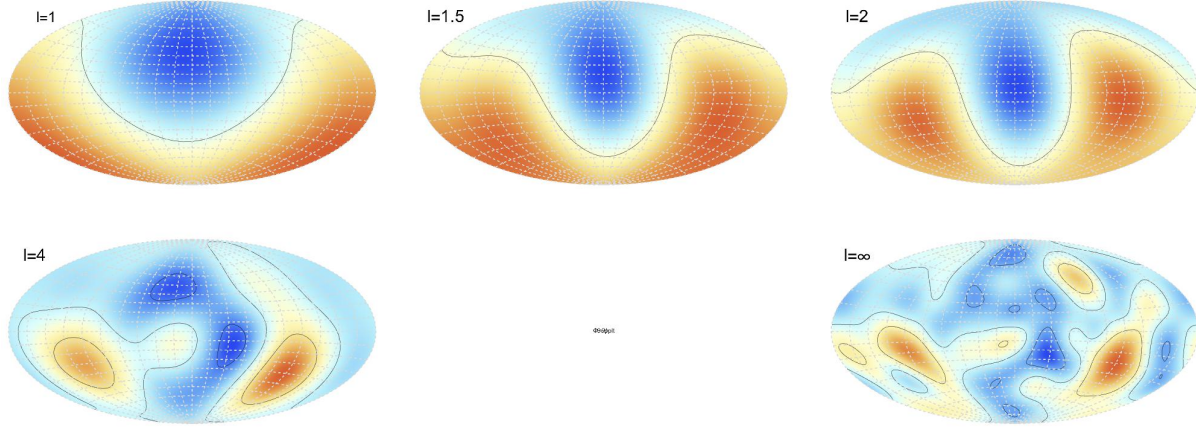


Figure 1. Aitoff projections of the potential on the cosmic photosphere $\Phi(\theta, \phi; \ell)$ at $x = 1$ for different angular resolutions, parametrized by ℓ . The contour levels are 0 ± 1 . A fixed set of random Fourier components truncated with $n_{max} = 3$ is used.

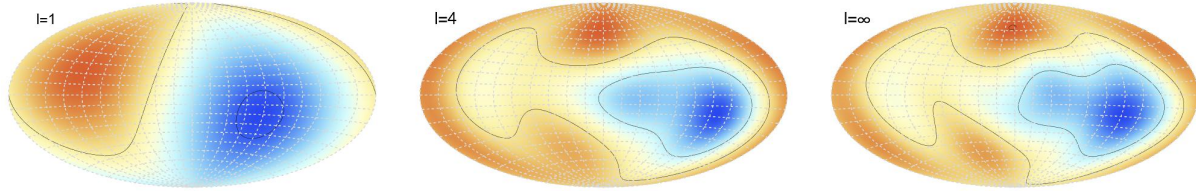


Figure 2. Aitoff projections of the potential on a sphere with $x = 0.5$ with the same Fourier series as in Fig. 1. The expansion up to $\ell = 4$ is a very good approximation to the full potential.

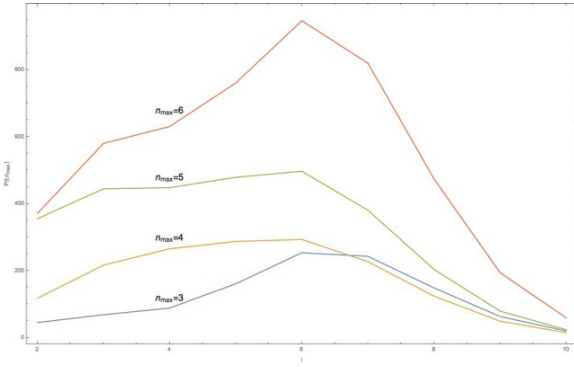


Figure 3. Importance of spherical harmonics of order ℓ for shells in k -space with inner radius $n_{max} - 1$ and outer radius n_{max} .

and the matrix S is diagonal, with elements $S_{nn} = \sigma_n^2$. Differentiating this expression leads to a set of linear equations which can be solved for the maximum posterior 3D potential Fourier coefficients \mathbf{f}_{MP} , given a choice of power spectrum normalisation α . We follow (Suyu et al. 2006) and infer the most probable normalisation α_{MP} using the Bayesian Evidence, which leads to the approximate condition

$$(\mathbf{a} - \mathbf{R}\mathbf{f}_{MP})^T C^{-1} (\mathbf{a} - \mathbf{R}\mathbf{f}_{MP}) + \mathbf{f}_{MP}^T S^{-1} (\alpha) \mathbf{f}_{MP} \approx N/2 \quad (9)$$

where N is the number of spherical harmonic coefficients used. An iterative scheme was used to optimize α in this way.

We note that the covariance matrix of the measured spherical harmonic coefficients should not include any cos-

mic variance terms, because we are interested in inferring the 3D potential in our one observable universe. To estimate this object, we took 100 posterior sample ‘‘Commander-Ruler’’ temperature maps, decomposed each of them into spherical harmonics,² and then calculated the sample variance and sample covariance of the coefficients.

6 DISCUSSION

References

Suyu, S. H., Marshall, P. J., Hobson, M. P., & Blandford, R. D. 2006, MNRAS, 371, 983

² We use the HEALPY code provided at <https://healpy.readthedocs.org>.